Polyurethane Doped with Low-Concentration Erbium

C. Ciobanu,[1] E. Stoica,[1] C. N. Cascaval,[1] D. Rosu,[1] L. Rosu,[1] M. State,[2] A. Emandi,[3] I. Nemes,[4] F. Petrescu[4]

[1]*Institute of Macromolecular Chemistry ''Petru Poni,'' Gr. Ghica Voda Alley, No. 41A, Iassy 700487, Romania*
[2]*Technical University ''Gh. Asachi'', D. Mangeron Avenue, No. 71A, Iassy 700050, Romania*
[3]*Bucharest University, Mihail Kogalniceanu Street, No. 64, Bucharest 050108, Romania*
[4]*SC INCERPLAST SA Bucharest, Ziduri Mosi Street, No. 23, Bucharest 023322, Romania*

Received 21 July 2005; accepted 28 November 2005
DOI 10.1002/app.23870
Published online in Wiley InterScience (www.interscience.wiley.com).

ABSTRACT: Polyurethane (PU) with lactate structures in its conformation can be used as a biological and biodegradable polymer. Polyurethane lactate (PUL) was doped with small quantities of an erbium (Er^{3+}) complex, which hindered the N=N group. 2,2′-Dihydroxyazobenzene was used as a ligand for the Er^{3+} complex. PUL in the presence of the used Er^{3+} complex caused water from the complex to be replaced by the polar structures from the polymer. These structures acted as crystallization germs for the structuration of the PU matrix. As a consequence, both the mechanical and thermal properties of the polymer were improved. The sample with the highest mechanical properties contained only 0.064 μmol of Er^{3+} complex/g of sample. © 2006 Wiley Periodicals, Inc. J Appl Polym Sci 103: 659–669, 2007

Key words: FTIR; matrix; mechanical properties; metal-polymer complexes; polyurethanes

INTRODUCTION

A lot of materials based on polyurethane (PU), such as foams, elastomers, adhesives, coatings, and sealants, have interested a broad spectrum of scientists with respect to their chemistry and physical properties. The development of nanostructurated, PU-based polymeric systems with important applications in electronics, medicine, aerospace, analytical chemistry and so on is a very attractive field for advanced polymeric materials. The introduction of metallic ions in various quantities in the PU matrix can change its processing, physicomechanical, thermal, electrical, and photochemical properties.[1–4] Great interest has surrounded the PU matrix doped with rare-earth ions.[5–8] Rare-earth elements have been used extensively as active ions in amplifiers and lasers.[9,10] The research and understanding of the interactions between rare-earth ions and urethane groups can constitute the starting base for the production of some new PU materials. These kinds of materials are especially used in electrooptical fields, where the structure of the polymeric matrix and its stability in time for different exploitation conditions are of major importance. In particular, erbium (Er^{3+})-doped fiber amplifiers have reached a stage of practical application in integrated optics.[11] Er^{3+}-doped long-chain diureasils, as high-transparent monoliths, are acceptable ion conductors[12] and behave like white-light phosphorous.[13] An important application that uses Er ions is Er-doped optical wave-guide amplifiers in inorganic matrices.[14]

To examine the nonlinear properties of the azo groups in the presence of electronic nonlinearity, this study was focused on the synthesis and characterization of a polyurethane lactate (PUL) doped with an organic Er^{3+} complex, which hindered the N=N group. Metal complexes with compounds containing nitrogen have potential applications in electrochemistry.[15] The electrooptical properties of Er complex systems can be influenced by their embedding into organic polymeric host matrices.[16]

The ligand for Er^{3+} was 2,2′-dihydroxyazobenzene (DAB). It was chosen as a ligand for Er^{3+} because our laboratory experiments showed that Er^{3+}–DAB complex possessed high luminescence properties. The lactate structure was introduced in the PU chain because materials obtained with lactate polymers are biodegradable and have biological activity.[17,18] Both the PUL and the Er^{3+} complex were soluble in dimethylformamide (DMF). The samples were analyzed with Fourier transform infrared (FTIR) spectroscopy, wide-angle X-ray scattering (WAXS), and mechanical and thermal property testing.

EXPERIMENTAL

Materials

The raw reactive compounds used for the synthesis of both PUL and the Er^{3+} complex were as follows:

Correspondence to: C. N. Cascaval (cascaval@icmpp.ro).
Contract grant sponsor: Romanian Ministry of Education and Research; contract grant number: C 3-126/2003.

TABLE I
PUL with Various Quantities of Er^{3+} Complex

Sample	Dry sample weight (%)	Er^{3+} complex	
		μg/g	μmol/g
Etalon	30.82	0	0
1	30.75	38.25	0.064
2	29.24	78.97	0.133
3	28.47	119.48	0.201
4	28.49	156.39	0.263
5	27.31	207.84	0.350
6	26.59	230.61	0.388

4,4′-diphenylmethane diisocyanate (MDI; 99.2% purity), ethylene glycol (EG; 98%), adipic acid (99%), diethylene glycol (DEG; 99%), racemic lactic acid (90%), DAB (97%), and erbium nitrate [$Er(NO_3)_3 \cdot 5H_2O$; 99.9%]. They were obtained from Sigma-Aldrich (Deisenhofe, Germany) and were used as received without further purification. The other compounds used in this study were analytical grades.

Synthesis of poly(diethylene adipate diol) (PDEA)

PDEA was synthesized by the fusion condensation of adipic acid with DEG (molar ratio = 1 : 1.08) in two stages: (1) the reaction between adipic acid and DEG with water elimination in the 160–180°C temperature range (time = 11 h) and (2) the transesterification reaction with 0.1 mol of DEG elimination at 220°C (2 mmHg vacuum, time = 1 h). The synthesized PDEA had a number-average molecular weight of 1800, which was determined from gel permeation chromatography (GPC). The PDEA was characterized by a hydroxyl number of 62 mg of KOH/g of polymer and an acidity index of 0.2 mg of KOH/g of polymer.

Synthesis of diethylene glycol lactate (DEGL)

DEGL was obtained by direct condensation between racemic lactic acid (1 mol) and DEG (1.66 mol). The reaction was carried out at a temperature of 160°C and a pressure of 5 mmHg for 2 h with continuous elimination of water. The synthesized DEGL had a molar mass of 180, a hydroxyl number of 622 mg of KOH/g of compound, and an acidity index of 0.022 mg of KOH/g of compound.

Synthesis of PUL

We obtained PUL by starting from PDEA (1 mol), DEGL (0.3 mol), MDI (3.6 mol), and EG (2.5 mL). PUL were synthesized by melt polymerization of the components at 80°C (time = 11 h). The solid PUL obtained had a concentration of urethane groups of 2.49 mol/1000 g of polymer and a number-average molecular weight of 58.500, as determined from GPC.

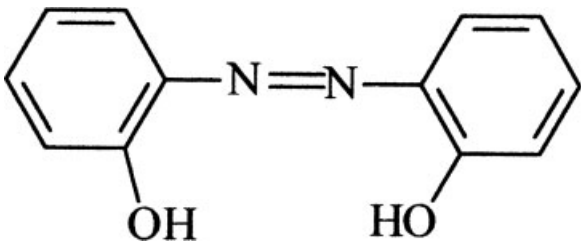

Figure 1 General formula of DAB.

Synthesis of the Er^{3+} complex

A mixture consisting of 0.25 g (1 mmol) of DAB, 0.223 g (0.5 mmol) of $Er(NO_3)_3 \cdot 5H_2O$, and 20 mL of H_2O was heated to reflux (time = 8 h). The starting mixture had a pH between 8.5 and 8.7. By means of a 5 wt % HCl solution, the pH was fixed at 6. The precipitate was filtered, washed with absolute ethanol, and purified by recrystallization. A product of dark red color (abridged Er^{3+}–DAB complex) was obtained (Yield: 52%). Elemental analysis:

ANAL. Calcd for $C_{24}H_{18}ErN_4O_4$: C, 48.55%; H, 3.06%; N, 9.44%; Er, 28.17%. Found: C, 48.24%; H, 3.09%; N, 9.26%; Er, 28.22%.

Preparation of the PUL–Er^{3+}–DAB complex mixture

PUL dissolved in DMF and taken as the dry substance was mixed with different quantities of the Er^{3+}–DAB complex, which was dissolved in the same solvent,

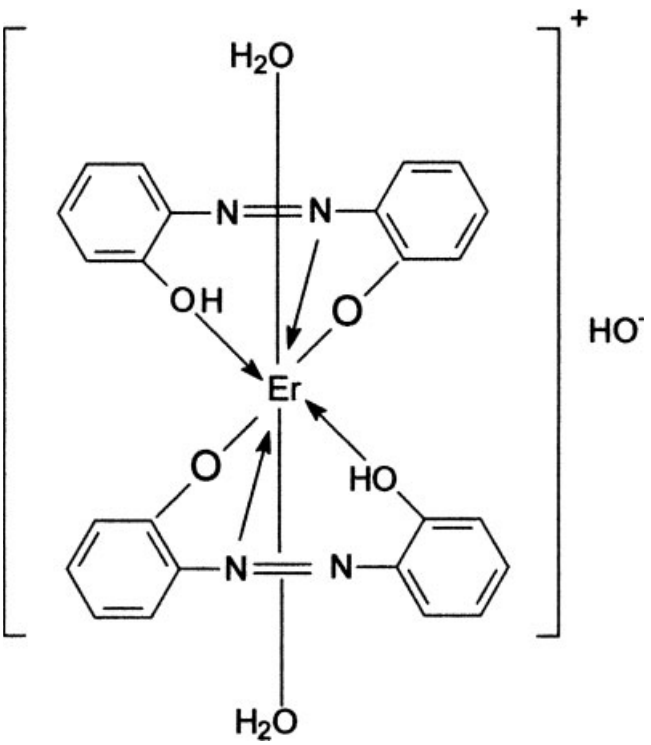

Figure 2 General formula of the Er^{3+}–DAB complex.

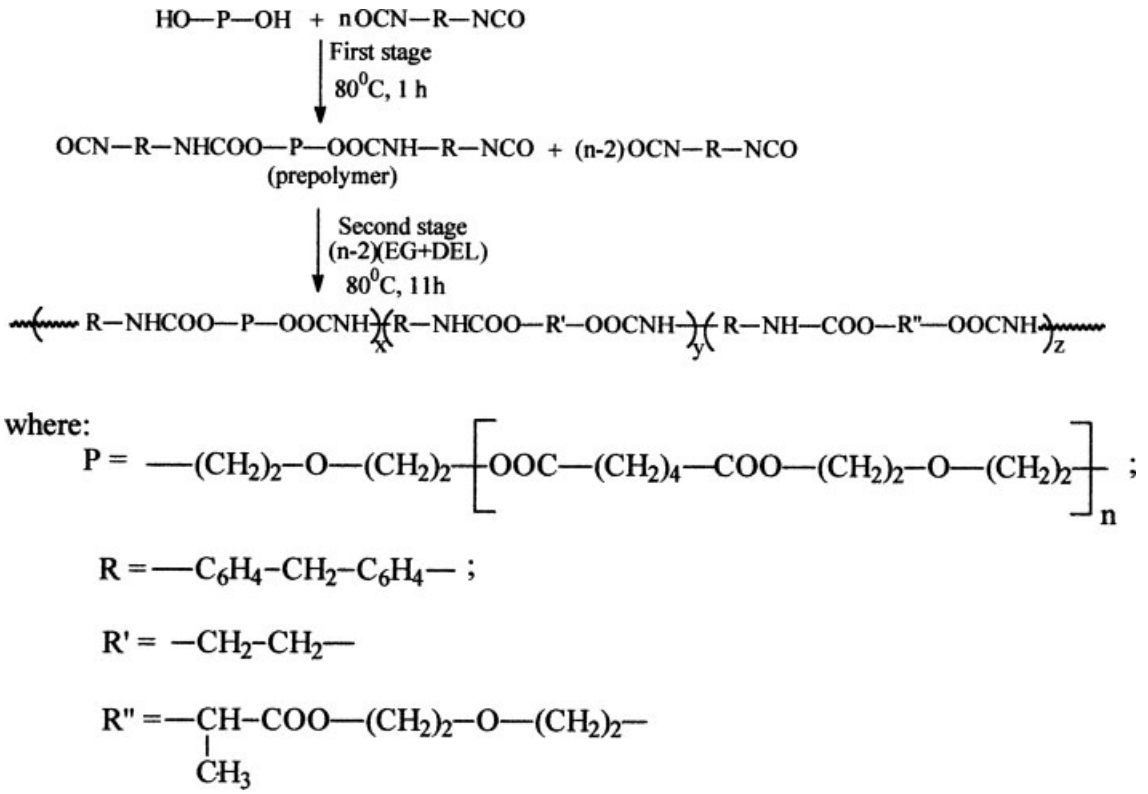

Scheme 1 Synthesis of PUL.

DMF. PUL standard substance and PUL–Er^{3+}–DAB complex samples (Table I) were cast as films on glass slides (220 × 240 mm) by means of doctor blading with a slit of 0.8 mm. The films were dried in an oven at 100°C under a pressure of 20 mmHg for 2 h. The films detached from the glass were conditioned in a desiccator at room temperature and a pressure of 1–2 mmHg for 1 week.

Characterization

GPC measurements were carried out with an PL-EMD-950 apparatus with an evaporative mass detector (Polymer Laboratories, Ltd., Shropshire, United Kingdom). Calibration of the apparatus was performed with monodispersing polystyrene standard samples with a narrow polydispersity (Polymer Laboratories, GmbH, Darmstadt, Germany).

The viscosity of the synthesized polymers was determined on a Brookfield-type viscosimeter (Brookfield Engineering Laboratories, Stoughton, Massachusetts), which was run at a speed of 6 rpm at 20°C.

The FTIR spectra of the synthesized samples were recorded on a Digilab Scimitar FTS-1000 spectrophotometer (Varian, Inc., Palo Alto, California) with KBr pellets.

Elemental analysis was carried out with Pregl's method. Er^{3+} was determined as a metallic ion by flame atomic absorption spectroscopy.

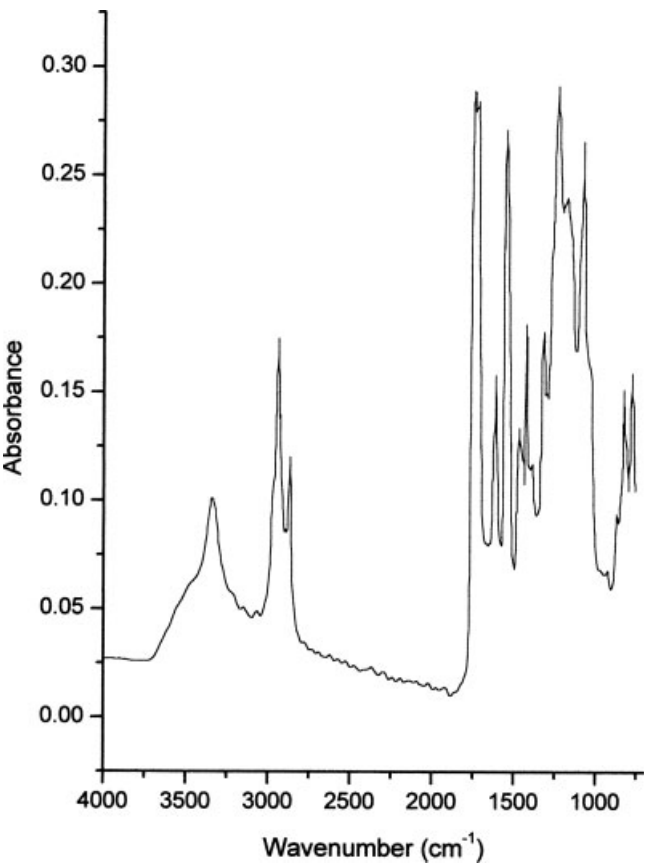

Figure 3 FTIR spectrum of PUL.

TABLE II
IR Characteristic Bands of PUL

Wavenumber, cm^{-1}	Assignments
3350	ν(N—H), free
3327	ν(N—H), H-bonded
2954	$\nu_{as}(—CH_3)$
2920	$\nu_{as}(—CH_2—)$
2850	$\nu_{s}(—CH_2—)$
1734	ν(C=O) in urethane and ester, free
1708	ν(C=O) in urethane and ester, H-bonded
1598	ν(C=C) in aromatic ring
1535	δ(N—H) and ν(C—N), amide II
1458	$\delta_{as}(—CH_3)$ and $\delta_{sciss}(—CH_2—)$
1413	$\delta_{sciss}(—CH_2—)$ adjacent to carbonyl
1381	$\delta_{s}(—CH_3)$
1309	δ(N—H) and ν(C—N), amide II
1066	ν_{as}(C—O—C), in ether
962	ν_{s}(C—O—C), in ether
817	γ(C—H), in aromatic ring
767	ω(N—H)

ν, stretching vibrations; δ, bending vibrations; γ, out of plane bending; ω, out of plane wagging; as, assymetrical; s, symmetrical; sciss, scissoring.

Thermogravimetry and derivative thermogravimetry (DTG) measurements were carried out with a MOM Q 1500-D derivatograph (MOM, Budapest, Hungary) under the following operational conditions: sample weight = 50 mg, heating rate = 12°C/min, atmospheric air, and α-Al_2O_3 reference material.

The physicomechanical measurements were carried out at room temperature with a TIRA-TEST-2161 apparatus (Tira, GmbH, Schalkau, Germany) at a crosshead speed of 20 mm/min coupled with a computer.

The WAXS analyses were performed on a TUR M-62 diffractometer (VEB TUR, Dresden, Germany) coupled with a computer, and Ni-filtered Cu K_2 radiation (λ = 0.154 nm) was used. The working conditions were 36 kV and 200 mA and a goniometer speed of 0.5°C/min. All the diffractograms were investigated in the range $2\theta = 4–40^\circ$ and room temperature. The crystalline part versus the amorphous part was evaluated with the regression method.

RESULTS AND DISCUSSION

Starting from DAB, with the general formula shown in Figure 1, we synthesized $Er(NO_3)_3 \cdot 5H_2O$ salt and the Er^{3+}–DAB complex.

Elemental analysis indicated that the complex of Er^{3+} with DAB could be formulated as M^+L (where M is the metal and L is the ligand). The data corresponded to a general formula $[Er(LH)_2OH] \cdot 2H_2O$. The disappearance of the OH band of the free ligand in the IR spectrum of the metal complex indicated that the OH group was deprotonated and coordinated to

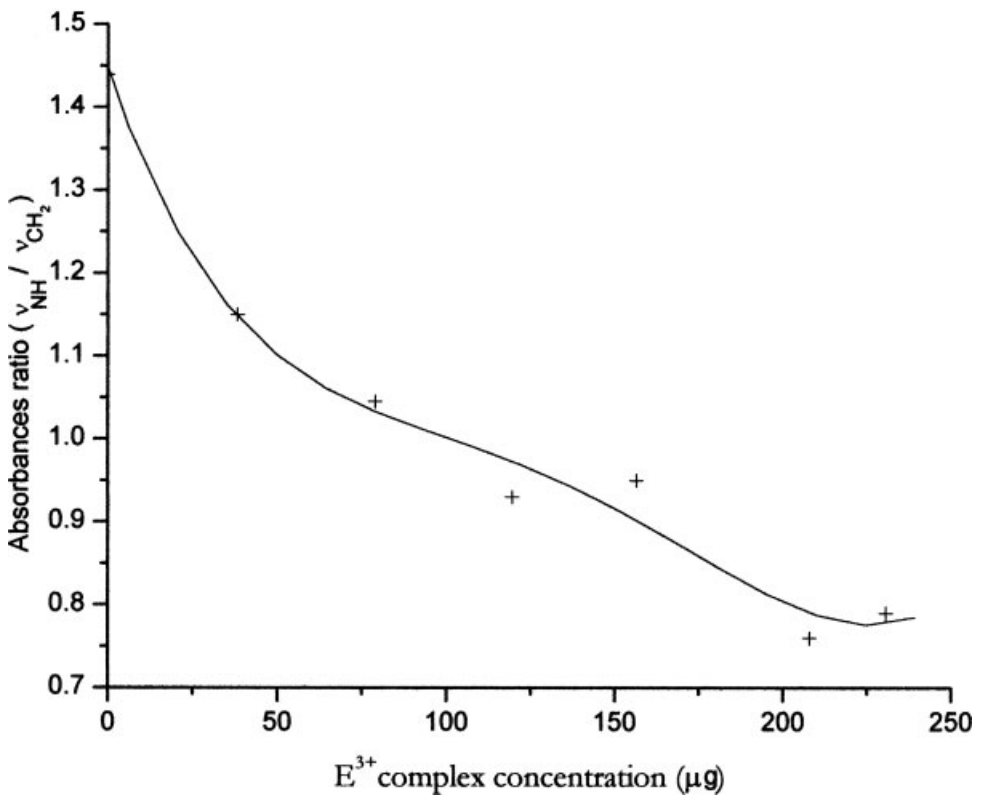

Figure 4 Change of ν(N—H)/$\nu_{as}(CH_2)$ absorbances ratio versus the Er^{3+} concentration.

the metal ion as —O. The IR results showed that the ligand was coordinated to Er^{3+} by means of both N and O. According to the aforementioned data, we propose for the synthesized complex the structure shown in Figure 2.

The complex used was an octacoordinated one containing two molecules of DAB and a trivalent Er ion as central ion, according to the common stereochemistry of this kind of compounds.[19]

PUL was obtained in two stages (Scheme 1) starting from PDEA, MDI (the first stage), EG, and DEGL (the second stage).

The ester, ether, and urethane dietilenelactate blocs ($x/y/z$ molar ratio = 1 : 2.5 : 0.3) were statistically distributed on the molecular chain.

FTIR analysis

The synthesized PUL was first characterized with FTIR spectroscopy, and the FTIR spectrum is shown in Figure 3.

The main wave numbers corresponding to the characteristic bands are shown in Table II.

Two spectral regions that are widely used to prove the coordination of the cations to the host polymer[20,21] were analyzed as follows: (1) the ν(N—H) absorbance from 3327 cm^{-1}, which is associated with the carbonyl group from ester and from urethane structures by means of p electrons, and $\nu_{as}(CH_2)$ absorbance band from 2920 cm^{-1} and (2) the skeleton band stretching of C=O groups from urethane and ester in the 1000–1300 cm^{-1} range.[22,23] The analysis of the absorbances showed that the peak of ν(N—H) from 3327 cm^{-1} decreased and shifted toward the higher wave numbers with approximately 10–15 cm^{-1}, whereas the $\nu(N—H)/\nu_{as}(CH_2)$ absorbance band ratio decreased with increasing Er^{3+} complex concentration. The experimental data presented in Figure 4 were approximated by the polynomial regression fourth-order polynomial.

The greatest decrease of the $\nu(N—H)/\nu_{as}(CH_2)$ ratio was remarked for sample 1, with 20% compared to the etalon sample, whereas samples 2–6 showed a lower decrease. In the range 1000–1300 cm^{-1}, the absorbance bands from 1252, 1224, 1176, 1145, and 1077 cm^{-1} were modified compared to the etalon sample. The shoulder from 1252 cm^{-1}, which was characteristic of the stretching vibration of the ν(O—C—N) band, combined with the deformation vibration δ(N—H) of the urethane groups with lower order, had the same intensity as the peak at 1224 cm^{-1}, specific to the urethane groups with higher order. Simultaneously, the absorbances that were characteristic of ν_{as}(C—O—C) at 1176 cm^{-1} from ester, ν_{as}(C—O—C) at 1145 cm^{-1} from urethane, and ν_{as}(C—O—C) at 1077 cm^{-1} from ether increased (Fig. 5). These transformations could be related to the accentuation of the phase separation from the polymeric matrix in the presence of the Er^{3+} complex, the doped PU being more ordered toward the etalon sample.

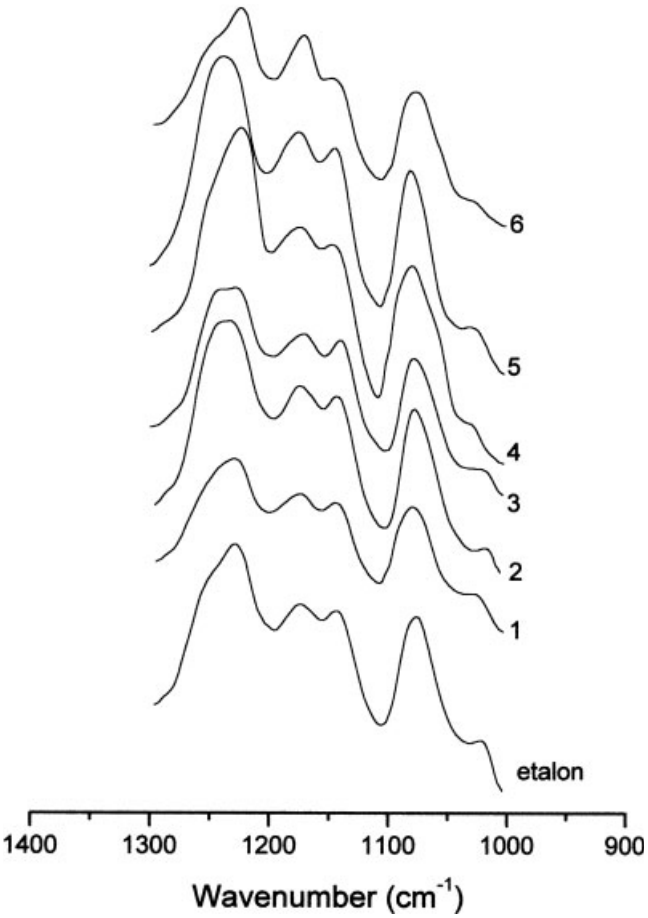

Figure 5 Skeleton absorbances of urethane, esterice, and etheric groups.

Because of the low concentration of Er^{3+} complex in the PUL sample, no visible transformations were observed in the polymer matrix by means of intermolecular and intramolecular interactions. This led us to suppose that the Er^{3+} complex molecules constituted the germs of formation, growth, and structuration of the microphases of both urethane–urethane and urethane–ester associations on the nanoscale level.

The introduction of the Er^{3+} complex into PUL was followed by the disappearance of the peak from 2350 cm^{-1}, which was specific to the metal–water bond.[24] This meant that the coordination water was replaced by the polar structures from the polymer, most probably from the urethane carbonyl,[7,8,25] as shown in Scheme 2.

WAXS analyses

The ordered domains both in the etalon and Er^{3+}-complex-doped samples were examined by means of

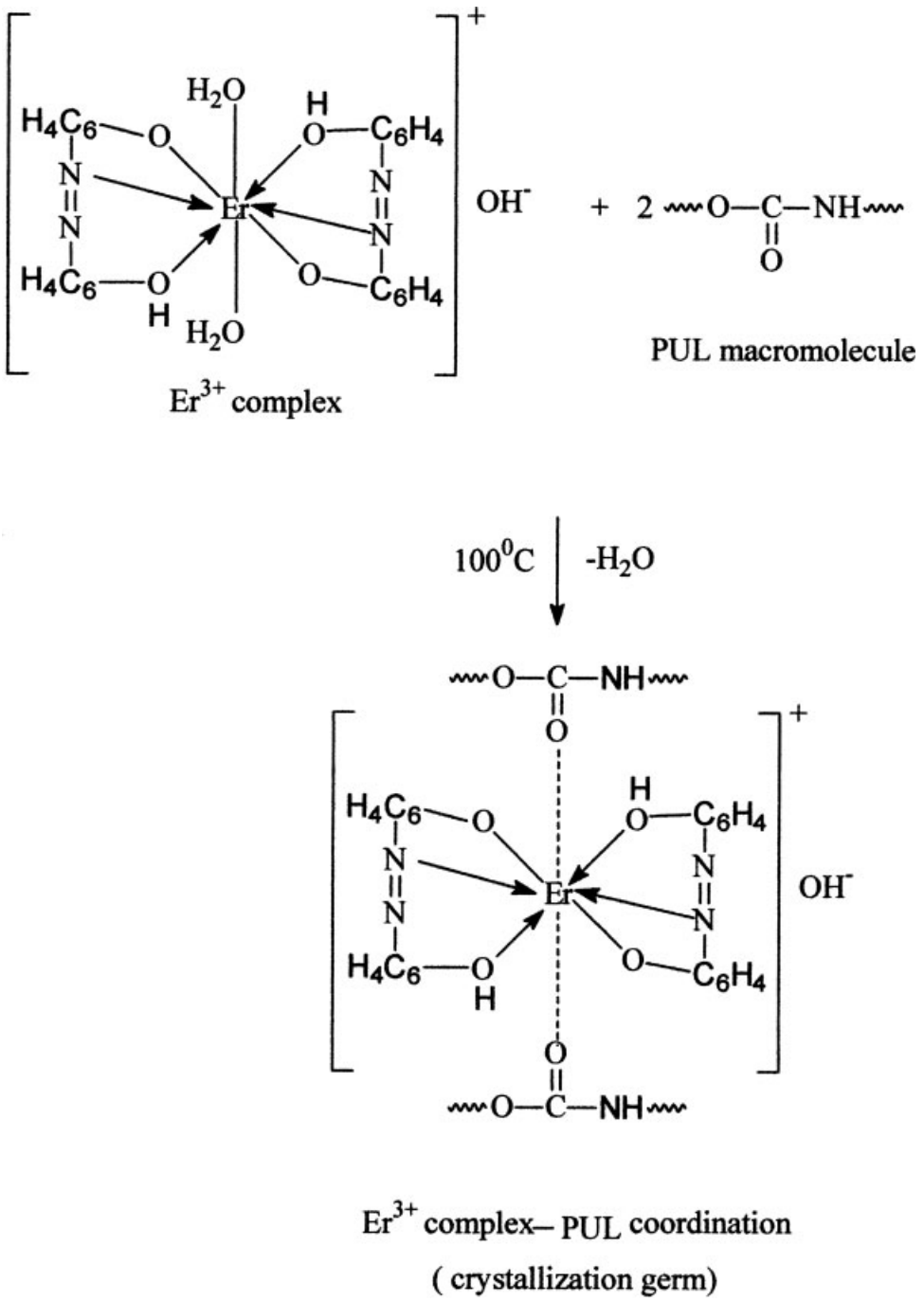

Scheme 2 Schematic diagram of the Er^{3+} complex with PUL structures.

WAXS, and Figure 6 shows the WAXS diffraction pattern recorded at room temperature.

Each WAXS diffraction pattern was characterized by two of the distinct crystal structures, type I and type II. Their proportion depended on both the chemical and supramolecular structure of PU. The type II crystal structures were more ordered than the type I structures. The curves shown in Figure 6 were used to evaluate the crystallinity index (α_x), as the ratio of the area under the crystalline zones (ΣA_{cr}) to the total scattering given by the sum between both the area of crystalline and amorphous zones (ΣA_{am}):[26–28]

$$\alpha_x = \frac{\sum A_{cr}}{(\sum A_{cr} + \sum A_{am})}$$

The areas were obtained by integration of the curves in the range $2\theta = 5$–35°. Table III lists the values of α_x for the studied samples and respective crystallinity indices of type I (α_{xI}) and type II (α_{xII}) crystal forms.

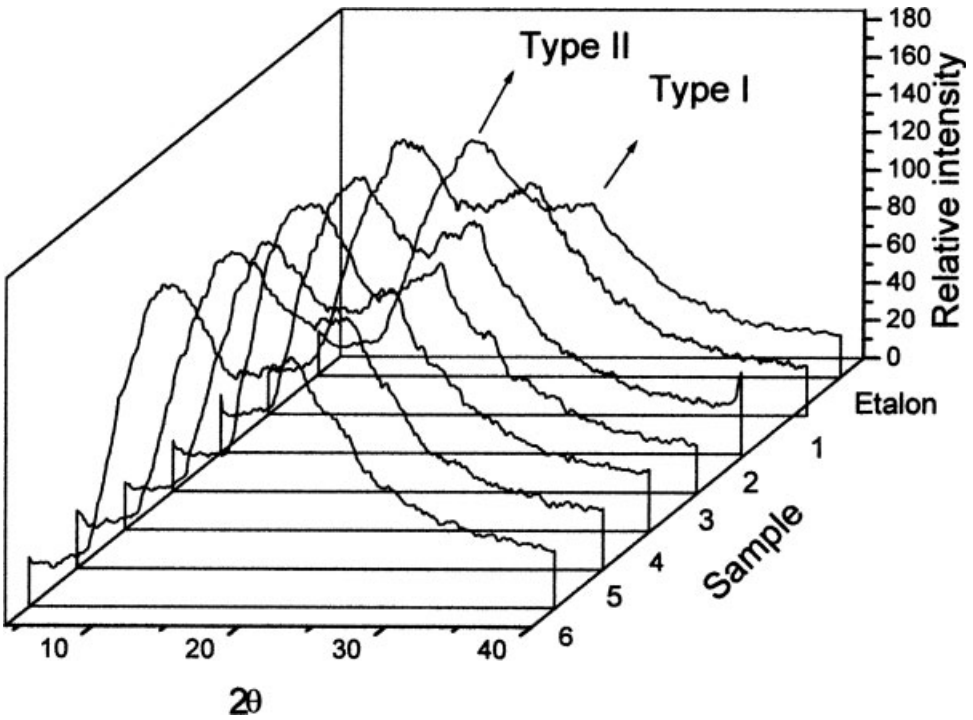

Figure 6 Diffractograms of the tested samples.

Both Figure 6 and Table III show that the α_x values proportionally increased with increasing Er^{3+} complex in the PU matrix, and α_{xII} was more pronounced than α_{xI}. The total crystallinity starting with sample 2 was about two times higher than the crystallinity of the etalon sample. This behavior led us to suppose that the large structures, such as —Ph—NH—COO—$(CH_2)_2$—O—$(CH_2)_2$—OOC—$(CH_2)_4$—, —Ph—NH—COO—$(CH_2)_2$—OOC—HN—Ph—, and —Ph—NH—COO—$(CH_2)_2$—O—$(CH_2)_2$—OOC—$CH(CH_3)$—OOCHN—Ph—, were better organized as clusters and well separated from the amorphous zones.

Physicomechanical analysis

Figure 7 shows the experimental curves obtained when we plotted the stress (σ) versus the strain (ε).

TABLE III
Crystallinity of the Studied Samples

Sample	α_{xI} (%)	α_{xII} (%)	α_{total} (%)	$\alpha_{relative}$
Etalon	1.3	3.36	4.66	1.00
1	2.90	3.26	6.16	1.32
2	4.30	4.62	8.92	1.91
3	4.24	6.92	11.16	2.39
4	4.58	5.16	9.74	2.09
5	3.46	4.46	7.92	1.69
6	4.69	4.96	9.65	2.07

$\alpha_{total} = \alpha_{xI} + \alpha_{xII}$; $\alpha_{relative} = \alpha_{total,sample}/\alpha_{total,etalon}$.

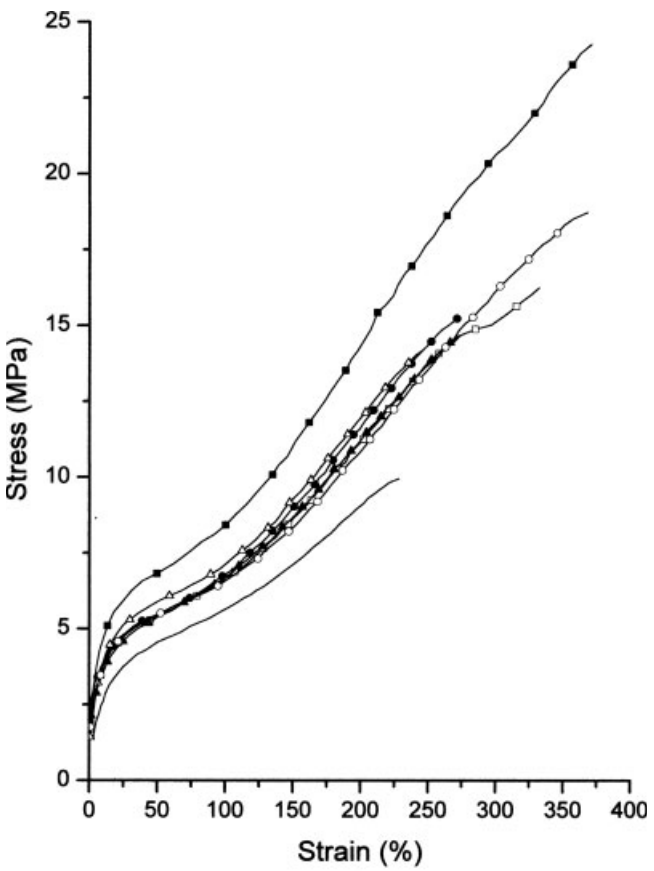

Figure 7 Dependency of σ versus the ε (δ–ε curves) for the studied samples: (—) etalon, (■) 1, (□) 2, (●) 3, (▲) 4, (△) 5, and (○) 6.

TABLE IV
Physicomechanical Properties of the Studied Samples

Sample	E at 100% strain (MPa)	U_e (MPa)	Break resistance (MPa)	ε at break (%)	D (MPa)
Etalon	5.74	0.08	10	228	1344
1	8.11	0.37	24	371	4634
2	6.66	0.26	16	332	1689
3	6.74	0.45	15	271	1718
4	6.66	0.21	14	273	1991
5	6.98	0.13	14	247	1888
6	6.41	0.28	14	248	3509

Some of the mechanical properties obtained for the tested samples are listed in Table IV.

Better mechanical properties were recorded for the doped PUL with Er^{3+} complex than the PUL etalon sample. The σ used for the ε of sample 1 was higher than that used for the ε of samples 2–6. The break resistance of sample 1 was 2.4 times higher than that of the etalon sample, whereas samples 2–6 were more resistant than the etalon sample by about 1.4–1.6 times. The elastic resilience (U_e), defined as a function directly proportional to σ^2 and inversely proportional to the double initial modulus of elasticity (E)

$$U_e = \frac{\sigma^2}{2E} \tag{1}$$

increased more for the doped samples than the etalon sample by about 1.6–5.6 times. This meant that the doped samples were more elastic, the internal mechanical work in the elastic domain increased, and the separation of phases were more accentuated.[28,29]

The durity (D), defined by the durity modulus, is the quantity of energy that is absorbed on the volume unity at the final ε. It is measured with the area under the σ–ε curve:

$$D = \int_0^{\varepsilon_f} \sigma_f d\,\varepsilon \tag{2}$$

where ε_f is the final strain in the maximum of the δ–ε curve and σ_f is the stress at the final stress in the maximum point of the δ–ε curve.

The data in Table IV show that D of the doped samples was greater than that of the etalon sample, and this supported the opinion of the structuration of the PU matrix as a consequence of its doping with the Er^{3+} complex.

Separation of the points on the σ–ε curves on the straight lines segments led to the observation that each curve was composed of eight straight lines, which were characterized by the slope and the cut-on ordinate (n'). This is well illustrated in Figures 8 and 9 for sample 1.

Each straight line corresponded to a morphological phase from the PUL matrix. The slope and n', which characterized E, were associated with the plastic strength of the respective morphological phase (Table V). The straight lines were plotted with the lower square method. All of the analyzed samples had the same number of straight lines, and this showed that

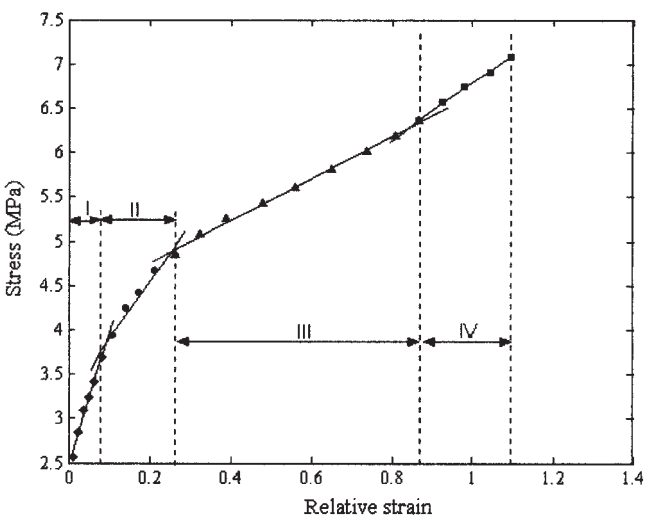

Figure 8 First four ε stages for the δ–ε curve.

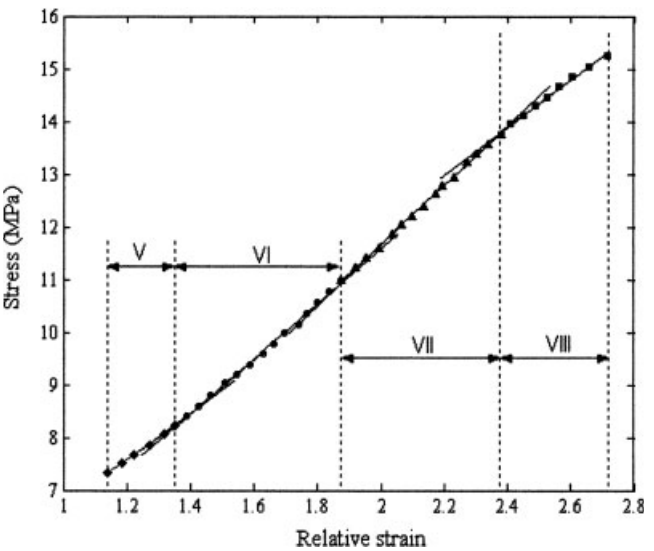

Figure 9 Last four ε stages for the δ–ε curve.

TABLE V
Values of *E* and *n′* for the Studied Samples

No. of straight lines	PUL–etalon		Sample 1		Sample 2		Sample 3		Sample 4		Sample 5		Sample 6	
	E (MPa)	*n′* (MPa)	*E* (MPa)	*n′* (MPa)	*E* (MPa)	*n′* (MPa)	*E* (MPa)	*n′* (MPa)	*E* (MPa)	*n′* (MPa)	*E* (MPa)	*n′* (MPa)	*E* (MPa)	*n′* (MPa)
1	24.34	0.67	29.25	1.95	19.91	1.88	33.95	1.22	21.79	1.73	22.69	1.72	15.21	2.47
2	13.92	1.20	5.66	4.45	9.75	2.56	16.23	2.22	6.28	3.22	8.40	2.91	5.81	3.38
3	5.82	2.30	3.18	5.20	4.10	3.56	6.77	3.44	2.21	4.33	3.87	3.73	2.29	4.33
4	2.45	3.26	5.12	3.20	2.63	4.03	2.41	4.63	3.61	2.90	2.35	4.22	2.98	3.81
5	2.56	3.08	6.62	1.07	3.73	2.93	3.80	3.30	5.19	0.48	4.36	2.11	4.21	2.51
6	3.22	2.27	6.41	1.68	4.84	1.41	5.00	2.50	5.32	0.26	4.96	1.23	5.29	1.02
7	3.87	1.28	5.72	3.48	5.18	0.87	5.52	2.90	4.60	2.27	1.49	10.58	5.59	0.47
8	3.51	2.03	5.52	3.87	4.66	2.03	4.15	3.97	3.23	6.88	3.55	4.40	4.27	3.67

no intermolecular and intramolecular crosslinkings took place in the PUL matrix doped with the Er^{3+} complex. Evolution of *E* for those eight straight lines showed that samples 1–6 were more homogeneous in the morphological state and more uniformly deformed than the PUL etalon sample.

Thermogravimetric analysis

The modification of both the weight (thermogravimetry) and the reaction rate (DTG) of the sample mass versus temperature is shown in Figures 10 and 11, respectively.

The DTG curves plotted for all of the studied samples showed the complexity of the degradation processes. Each sample was decomposed after various mechanisms. In the 200–340°C decomposition stage, there were differences regarding the intensity, position, and number of the peaks for each sample. This behavior led to assumption that the introduction of the Er^{3+} complex in the polymeric matrix formed different supramolecular structures, which presented various thermal decomposition kinetics. With the

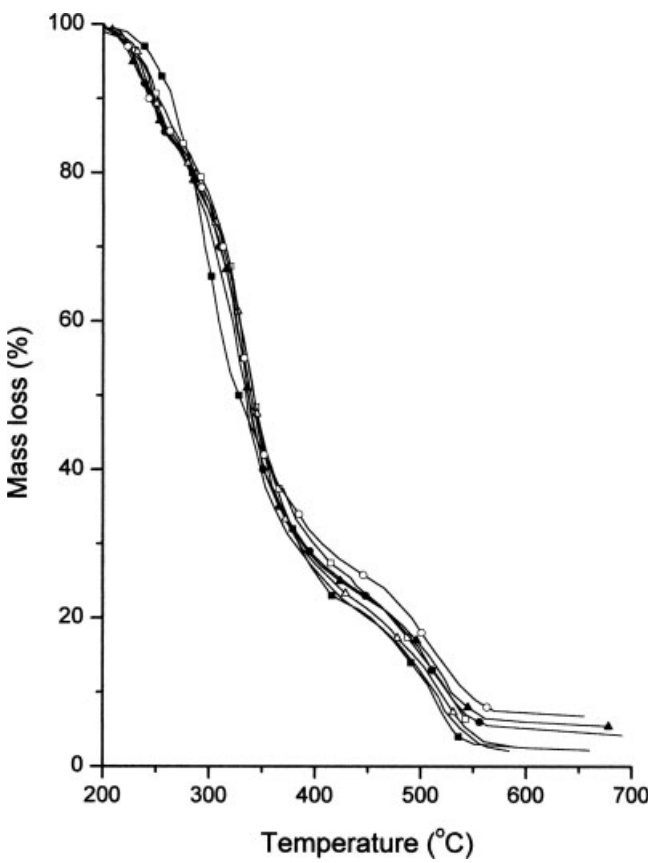

Figure 10 Dependency of mass loss versus temperature: (—) etalon, (■) 1, (□) 2, (●) 3, (▲) 4, (Δ) 5, and (○) 6.

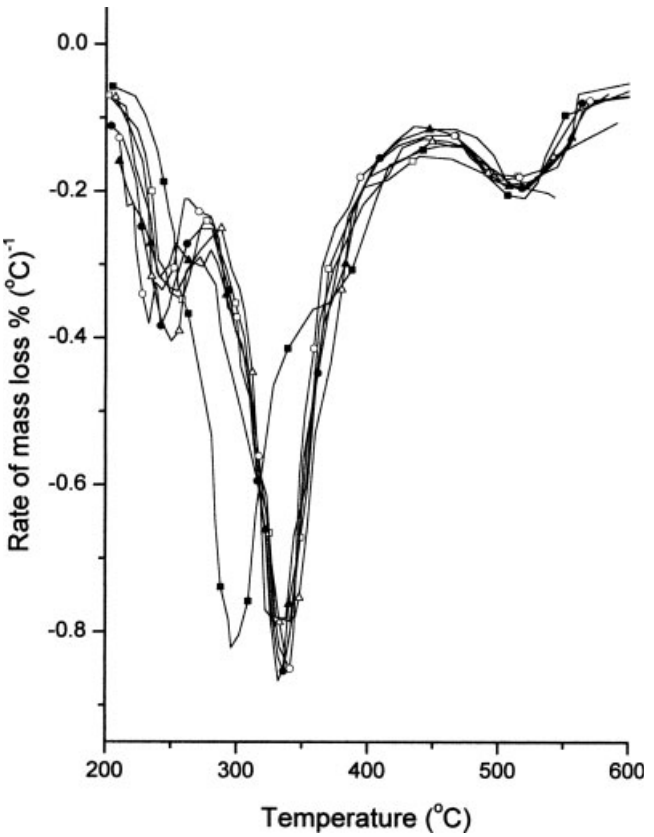

Figure 11 Dependency of the change rate of the sample versus temperature: (—) etalon, (■) 1, (□) 2, (●) 3, (▲) 4, (Δ) 5, and (○) 6.

TABLE VI
Some Kinetic Parameters Determined for the Studied Samples

	n		E_a (kcal/mol)	
Sample	200–270°C (I)	270–340°C (II)	200–270°C (I)	270–340°C (II)
Etalon	1.2	1.5	24	14
1	1.6	2.0	28	23
2	1.1	1.4	23	13
3	1.1	2.0	29	17
4	0.9	1.9	24	13
5	1.0	2.0	26	14
6	1.0	2.0	34	14

Coats–Redfern method,[30] both the medium reaction order (n) and the apparent activation energy (E_a) were evaluated for two decomposition stages, 200–270°C (stage I) and 270–340°C (stage II), and the values obtained for those two kinetic parameters are listed in Table VI.

E_a for the first analyzed stage showed a general tendency to increase, and n had values around 1 (with the exception of sample 1). Taking into consideration the initial decomposition temperature, we can say that the polymers doped with the Er^{3+} complex were more stable than the etalon sample. The kinetic parameters determined showed that the dissociation, transposition, cycloaddition, and transesterification reactions differed with proportion for the doped samples versus the etalon sample. This behavior was not due to the amount of Er^{3+} complex used but rather to the structuration process of the PUL sample. The n values around 1 indicated the presence of both the transposition and addition reactions with formation of urea, and birespective trimolecular cycloadditions as predominant against the condensation processes. In the 270–340°C decomposition stage, E_a had the general tendency to decrease with increasing Er^{3+} complex amount, and n had a medium value around 1.8. This meant that the nucleophile substitution reactions became predominant in this stage. It is possible for the Er^{3+} complex to play the role of catalyst in these kinds of reactions.

CONCLUSIONS

PU is a versatile material with important applications in advanced technologies. The lactate structures introduced in the PU matrix lead to biological and biodegradable materials. PU in the presence of rare-earth elements is extensively used as a good material for amplifiers and lasers. Metal complexes with compounds containing nitrogen have potential applications in electrochemistry.

PUL doped with the Er^{3+} complex, which hindered the N=N group, was studied with FTIR spectroscopy, X-ray analysis, and mechanical and thermal property testing. DAB was used as a ligand for Er^{3+}. The Er^{3+}–DAB complex possessed high luminescence properties.

The Er^{3+} complex caused the coordination water from the complex to be replaced by the urethane polar structures from PUL. These structures could be considered the crystallization germs for structuration of the PUL matrix. The presence of both the supramolecular structures in PUL and its structuration due to the used Er^{3+} complex led to improved mechanical properties and an increased thermal stability.

References

1. Ciobanu, C. Ph.D. Thesis, ''Petru Poni'' Institute of Macromolecular Chemistry, Iassy, Romania, 1979.
2. Palamaru, M.; Rusu, I.; Pruna, I.; Ciobanu, C. Thermochim Acta 1994, 235, 217.
3. Moroi, G.; Ciobanu, C. J Anal Appl Pyrolysis 2003, 70, 87.
4. Iordan, A. R.; Palamaru, M.; Cecal, A.; Popa, A. F.; Ciobanu, C.; Craus, M. I. J Polym Mater 2004, 53, 157.
5. Ryszkowska, A.; Gonçalves, M. C.; de Zea Bermudez, V.; Ostrovskii, D.; Carlos, L. D. J Macromol Struct 2002, 611, 83.
6. Silva, M. M.; de Zea Bermudez, V.; Carlos, L. D.; Passos de Almeida, P.; Smith, M. J. J Mater Chem 1999, 9, 1735.
7. de Zea Bermudez, V.; Ostrovskii, D.; Lavoryk, S.; Gonçalves, M. C.; Carlos, L. D.; Sa Ferreira, A. R.; Reis, L.; Jacobsson, P. Phys Chem Chem Phys 2004, 6, 638.
8. Gonçalves, M. C.; de Zea Bermudez, V.; Ostrovskii, D.; Carlos, L. D. Electrochim Acta 2003, 48, 1977.
9. Diagonnet, M. J. F. Rare Earths Doped Fiber and Amplifiers; Marcel Dekker: New York, 1993.
10. Snitzerm, E.; Koester, K. J Appl Opt 1996, 3, 1182.
11. Sejka, M.; Varming, P.; Hiibner, J.; Kristensen, M. Electron Lett 1995, 31, 1495.
12. Silva, M. M.; Silva, C. Y.; Smith, M. Y.; Assunçáo, M.; Aleácer, I. J Alloys Compd 1998, 275, 21.
13. Carlos, L. D.; Messaddeq, J.; Brito, H. F.; SáFerreira, R. A.; de Zea Bermudez, V.; Ribeiro, Y. L. Adv Mater 2000, 12, 594.
14. Polman, A.; Kik, P. G. MRS Bull 1989, 4, 48.
15. Hamada, Y. J. IEEE Trans Electron Devices 1997, 44, 1208.
16. Koppe, M.; Brabec, C. J.; Saricifter, N. S.; Eichen, Y.; Nakhmanovich, G.; Ehrenfreund, T.; Epstein, O.; Heiss, W. Synth Met 2001, 121, 1511.
17. Gunatillake, P. A.; Adhikari, R. Eur Cell Mater 2003, 5, 1.
18. Tura, V.; Apostu, M. O.; Melnig, V.; Ciobanu, C.; Hagiu, B. A. Timisoara Med J 2003, 53, 127.
19. Bauer, H.; Blanc, J.; Ross, D. L. J Am Chem Soc 1964, 86, 5125.
20. Berson, A.; Lindgren, J.; Huang, W.; Frech, R. Polymer 1995, 36, 4471.

21. Rey, I.; Lassegnes, J. C.; Gronding, J.; Servant, I. Electrochim Acta 1998, 43, 1505.
22. Tanaka, T.; Yokoyama, Y.; Yamaghuchi, Y. J Polym Sci Part A-1: Polym Chem 1968, 6, 2137.
23. Shen, D. Y.; Pollack, S. K.; Hsu, S. L. Macromolecules 1989, 22, 2564.
24. Parker, D.; Dickins, R. S.; Puschmann, H.; Crossland, C.; Howard, J. A. K. Chem Rev 2002, 102, 1977.
25. Liu, Q.-D.; Li, J.-R.; Gao, S.; Ma, B.-Q.; Liao, F.-H.; Zhou, Q.-Z.; Yu, K.-B. Inorg Chem Commun 2001, 4, 301.
26. Briber, R. M.; Thomas, E. L. J Polym Sci Part B: Polym Phys 2003, 23, 1915.
27. Pompe, G.; Polders, A.; Pötschke, P.; Pionteck, J. Polymer 1998, 39, 5147.
28. Ciobanu, C.; Xiaozu, H.; Cascaval, C. N.; Fengchun, G.; Rosu, D.; Ignat, L.; Moroi, G. J Appl Polym Sci 2003, 87, 1958.
29. Van Bogart, J. W.; Gibson, P. E.; Cooper, S. L. J Polym Sci Polym Phys Ed 1983, 21, 65.
30. Coats, A. W.; Redfern, I. P. Nature 1964, 35, 1464.